Light-Weight Free-Standing Carbon Nanotube-Silicon Films for Anodes of Lithium Ion Batteries

Li-Feng Cui,† Liangbing Hu,† Jang Wook Choi, and Yi Cui*

Department of Materials Science and Engineering, Stanford University, Stanford, California 94305. †These authors contributed equally to this work.

ABSTRACT Silicon is an attractive alloy-type anode material because of its highest known capacity (4200 mAh/g). However, lithium insertion into and extraction from silicon are accompanied by a huge volume change, up to 300%, which induces a strong strain on silicon and causes pulverization and rapid capacity fading due to the loss of the electrical contact between part of silicon and current collector. Si nanostructures such as nanowires, which are chemically and electrically bonded to the current collector, can overcome the pulverization problem, however, the heavy metal current collectors in these systems are larger in weight than Si active material. Herein we report a novel anode structure free of heavy metal current collectors by integrating a flexible, conductive carbon nanotube (CNT) network into a Si anode. The composite film is free-standing and has a structure similar to the steel bar reinforced concrete, where the infiltrated CNT network functions as both mechanical support and electrical conductor and Si as a high capacity anode material for Li-ion battery. Such free-standing film has a low sheet resistance of ~30 Ohm/sq. It shows a high specific charge storage capacity (~2000 mAh/g) and a good cycling life, superior to pure sputtered-on silicon films with similar thicknesses. Scanning electron micrographs show that Si is still connected by the CNT network even when small breaking or cracks appear in the film after cycling. The film can also "ripple up" to release the strain of a large volume change during lithium intercalation. The conductive composite film can function as both anode active material and current collector. It offers ~10 times improvement in specific capacity compared with widely used graphite/copper anode sheets.

KEYWORDS: lithium ion battery · silicon anode · carbon nanotube · composite structure · free-standing film · strain relaxation

Because of their high energy and power density, lithium ion batteries that were mainly used for portable electronics are now extending to large applications such as power tools and vehicle electrification. Extensive research has been carried out to find new electrode materials and new electrode structure designs to improve energy densities for both anode and cathode. Silicon as an anode material has attracted extensive research because it has the highest known capacity, more than 10 times the value of the current commercial graphite anode. However, the intrinsic volume expansion and contraction of Si during Li cycling cause rapid capacity fading and limit its wide application. Various approaches have been carried out to overcome this issue, including the use of nanosized active materials,[1−6] active/inactive composite materials,[7−9] and silicon−carbon composites.[9−14] These studies have resulted in improvements of the electrochemical performance of Si-based anodes, but only to a limited extent. Recently we found silicon nanowires directly grown on a current collector can greatly improve the performance of the Si anode due to the excellent electrical connection between Si nanowires and the current collector and the nature of one-dimensionality to effectively release the strain.[15,16] Cho and coworkers also demonstrated great anode performance using carbon-coated, very small (≤10 nm) silicon nanoparticles (SiNPs) or silicon nanotubes.[17,18] However, in these nanosilicon electrodes, the heavy current collector is larger in weight than Si active material. In a commercial lithium ion cell, the anode material is usually coated on a copper foil current collector to form an anode electrode in thin sheet form. The metal current collector on the anode side is usually a 10 μm thick copper sheet with an areal density ~10 mg/cm^2. This copper sheet is a relatively heavy component in a lithium ion cell, which is comparable in weight to the anode active material and accounts for ~10% of the total weight of the cell.[19]

Random networks of carbon nanotube (CNT) have been explored as transparent electrodes in various devices including solar cells, organic light emitting diodes, and smart windows, where CNT networks show optical transmittances of ~80% and sheet resistances of 100−1000 Ohm/sq.[20−25] Recently, we reported the replacement of the conventional metal current collector with lightweight, CNT-enabled conductive paper, which can significantly reduce the weight of Li-ion batteries.[19,26] Inks of CNT

*Address correspondence to yicui@stanford.edu.

Received for review March 26, 2010 and accepted May 25, 2010.

10.1021/nn100619m

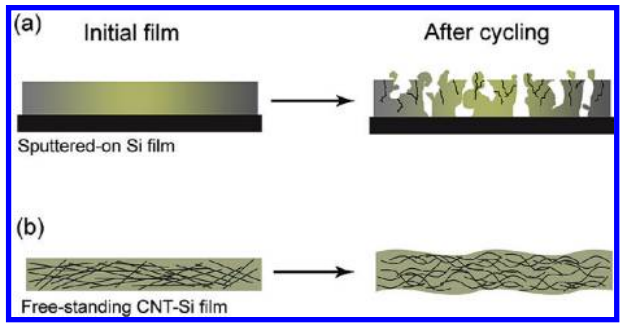

Figure 1. (a) Sputtered-on Si film tends to pulverize after Li^+ cycling. (b) CNT-Si films can "ripple up" to relax the large strain during Li^+ cycling.

or silver nanowire are printed on thin commercial paper that renders a highly conductive paper current collector for both the anode and the cathode of Li-ion batteries. In the current study, we report a new free-standing Si film approach, not only to release effectively the strain built up in high capacity Si anode through a new, different mechanism than Si nanowires, but also to eliminate the dead weight of heavy metal current collector. A lightweight and highly conductive and flexible CNT network effectively functions as both a mechanical support and an embedded-in current collector. The composite film has a structure similar to steel bar reinforced concrete, where the CNT network is infiltrated in the Si film and provides good conductivity and flexibility, as well as mechanical strength. The Si in the CNT-Si film can be either amorphous Si from SiH_4 CVD or crystalline SiNPs. Ripples were found to form after battery cycling. These ripples are believed to be critical to releasing the large strain in the Si anode during Li^+ insertion and extraction. Such bifunctional, free-standing film as both anode-active material and current collector leads to an extremely high energy density for anode electrodes, that is, 10 times the energy density is achieved when compared with the graphite/copper combination.

RESULTS AND DISCUSSION

Stainless Mesh Supported CNT-Si films. A number of previous studies have investigated Si films as the anode for lithium ion batteries,[27−30] where Si was deposited on metal substrates (current collector) by various sputtering methods. When very thin Si film is used, the strain in Si induced by lithium intercalation is relatively small and pulverization is limited. Great cycling performance (>200 cycles) has been obtained on very thin (thickness <500 nm), sputtered-on a-Si films.[27] However, the low material loading density per unit area of these very thin films has prevented their practical application. When relatively thick Si films (thickness > 2 μm) were used, fast capacity fading was observed.[27] This is because the large strain in the thick Si film during Li^+ cycling severely pulverizes the film and causes loss of contact of part of the Si with the substrate, as illustrated in Figure 1a. Yin *et al.*[28] have sputtered relatively thick a-Si film (thickness >2 μm) on a roughened copper substrate and obtained improved performance. They attributed this improvement to the reduction of strain in Si during Li^+ cycling on a roughened surface. In this report, we have synthesized a CNT-Si composite film for the anode of lithium ion batteries. CNTs are infiltrated in a Si film and function as a structural reinforcement and also a conductive network. The composite film has a structure similar to steel bar reinforced concrete, showing great strength and flexibility. This composite film can be made either on stainless steel (SS) mesh or free-standing. The good flexibility allows the film to "ripple up" to relax the large strain during Li^+ cycling, as indicated in Figure 1b. Relatively thick CNT-Si composite films up to 4 μm still show good cycling performance. In these composite films, CNT contributes less than 15% of the overall mass and Si is the major component. We can also stack multiple layers of these CNT-Si films as anode and obtained high active material loading density per unit area. Two layers of this composite film with a total thickness of 8 μm will have an area capacity larger than 2 mAh/cm^2, meeting the commercial standard.[19,26]

To demonstrate the feasibility of CNT-Si films as effective anode material, we first made a CNT-Si composite film on a SS 500 mesh, as shown by the SEM image in Figure 2a (see Experimental Section for detailed procedures). The SEM image clearly shows a film (or membrane) lying on the SS grids. Figure 2b is a zoom-in SEM image of the film, where CNT induced wire structures can be identified although the spaces between wires are filled with a-Si forming a continuous film. The inset image in Figure 2b is a selected area electron diffraction (SAED) image of the film. No crystalline diffraction pattern is observed for this film indicating the deposited Si is amorphous in nature. No clear CNTs can be seen in a typical TEM image of a ~1 μm thick CNT-Si film supported by a SS mesh because the majority of film content is a-Si. Figure 2c is a SEM image of a broken CNT-Si film, where CNTs can be clearly seen connecting the two broken pieces. From the image, even when the composite film is broken to a certain degree, the broken pieces are still connected by a CNT network. This behavior is exactly similar to the steel bar reinforced concrete, where the steel bar provides flexibility and extraordinary fracture resisting strength. All the tests were measured with pouch-type cells and using constant current charge and discharge with a voltage range of 1.0−0.01 V. The cycling rates were calculated according to the theoretical capacity of silicon (4200 mAh/g) and CNTs (~400 mAh/g), with a mass ratio of 6:1, where the overall theoretical capacity is ~3600 mAh/g and $1C = 3.6$ A/g. Figure 2d is a half cell test of an electrode made of SS mesh supported CNT-Si film. The first 12 cycles were cycled at a rate of *C*/10, and then the rate was increased to *C*/3 for the following cycles. The cell exhibits a good first cycle Coulombic efficiency of 84%

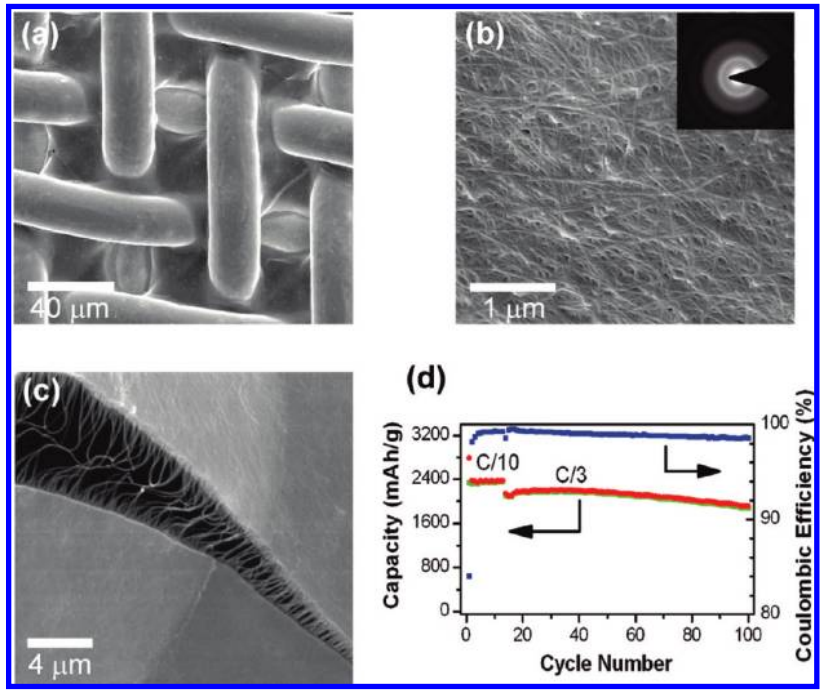

Figure 2. (a) SEM image of a CNT-Si film supported by a SS 500 mesh. (b) Zoom-in SEM of Figure 1a. Inset is a SAED image of the film. (c) SEM image of a broken film supported by SS mesh. (d) Charge (red) and discharge (green) capacity and Coulombic efficiency (blue) *versus* cycle number for a half cell using a SS mesh supported CNT-Si film as the working electrode cycled between 1−0.01 V.

and high efficiency, 98.5−99.8%, after the first few cycles. There is a capacity drop of about 11% when the cycling rate was increased from *C*/10 to *C*/3. The cell has a capacity retention of 90% after 90 cycles at a rate of *C*/3. It should be noticed here that it only takes the cell ~1.8 h to charge or discharge at a rate of *C*/3 because the CNT-Si film has a capacity of ~2000 mAh/g, and the cycling rate was calculated according to the theoretical capacity of 3600 mAh/g. The high specific capacity and excellent cycling performance confirmed that the CNT-Si film supported by SS mesh is an effective structure for Li-ion anodes.

Free-Standing CNT-Si Films. To improve the energy density of Li-ion battery devices, it is essential to decrease the weight contribution from each component. The high conductance of CNT films, ~5 Ohm/sq, could effectively replace the heavy current collector to achieve a current-collector-free Li-ion battery. To demonstrate the bifunctionality of our structure as both current collector and active anode material, free-standing CNT-Si film without SS mesh was fabricated (see Experimental Section for detailed procedures and Figure S1). Figure 3a shows a photograph of a free-standing CNT-Si composite film. The film is highly conductive after Si coating, ~30 Ohm/sq sheet resistance, and flexible, that is, it does not break upon bending. A cross section SEM image of the free-standing CNT-Si film indicates that it is ~4 μm in thickness. Figure 3b shows the cycling performance of a ~4 μm thick free-standing CNT-Si film at a rate of *C*/10. The discharge capacity is 2083 mAh/g at the beginning and remains 1711 mAh/g (or 82%) after 50 cycles. The Coulombic efficiency is 86% for the first cycle and greater than 98% throughout the rest cycles. We also stacked multiple layers of these CNT-Si films as anode and obtained higher active material loading density per unit area. Figure 3c shows the performance of an electrode using two layers of 4 μm thick CNT-Si films at a cycling rate of *C*/15. This cell shows good Coulombic efficiency and has a capacity retention of ~80% after 50 cycles. A four-layer stack of CNT-Si films was also tested and still demonstrated good performance (see Figure S2). Figure 3d is the voltage profile of a half cell using free-standing single layer CNT-Si film as the working electrode. The first charge has a long plateau at 0.18 V up to 1200 mAh/g, which is the first lithiation potential of pure a-Si.[27,31] The sloping region between 1200 and 2415 mAh/g is the further lithiation of amorphous Li_xSi. Because the first charge did not reach the formation of crystalline $Li_{15}Si_4$ (3579 mAh/g), the first discharge shows no plateau that could be originated from the delithiation of crystalline $Li_{15}Si_4$, as observed by previous studies.[15,32] After the first cycle, the charging and discharging profiles show typical behavior (sloping curves) of Li intercalating with amorphous Li_xSi.[16,31,32] The average charge potential is ~0.18 V and average discharge potential ~0.4 V, rendering a low average overpotential of ~0.11 V, suggesting that CNT-Si film is a good anode material with low charge/discharge voltage hysteresis. When compared with our previous work of Si coated on carbon nanofiber as anode, CNT-Si is much more flexible and can be made free-standing due to the excellent flexibility of the CNT

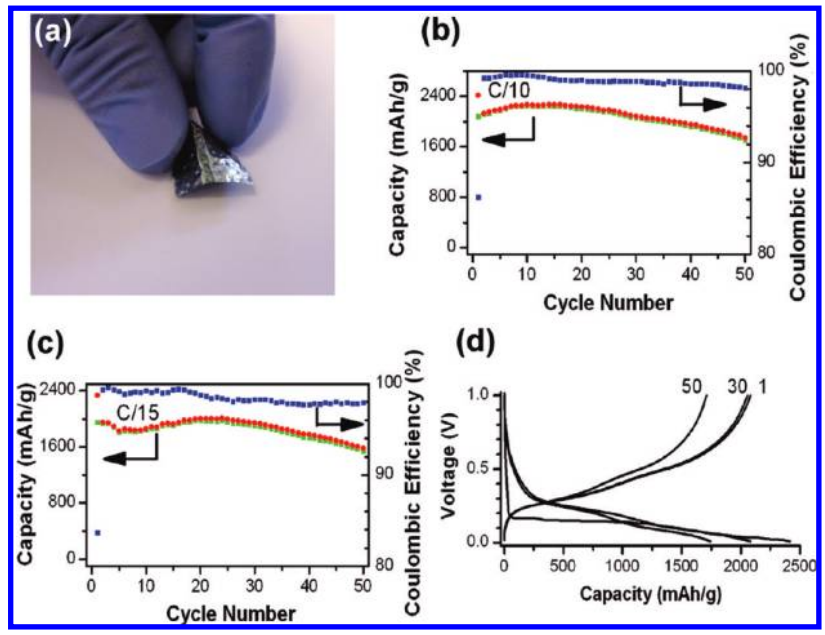

Figure 3. (a) Photograph of a free-standing CNT-Si film. (b,c) Charge (red) and discharge (green) capacity and Coulombic efficiency (blue) *versus* cycle number for a half cell using free-standing CNT-Si films as the working electrode cycled between 1−0.01 V, where (b) uses a single-layer, free-standing film and (c) uses two layers of free-standing films. (d) Voltage profile of the cell in (b).

network.[16] Furthermore, CNTs remain intact after battery cycling, which helps maintain the electrical connection between CNTs and Si. As discussed later, such bifunctional, free-standing CNT-Si anodes will largely improve the energy density of the Li-ion battery.

Incorporation of SiNPs into the CNT-Si Films. A relatively long CVD of 30 min was needed to fabricate the CNT-Si structure for bifunctional anodes. For practical, large-scale energy storages with low cost, solution processing is preferred against a high cost, vacuum-based process. This motivated us to investigate a solution-based process to incorporate Si nanoparticles into CNT films. Aqueous CNT-SiNP ink was prepared with a mass ratio of 6:1 and coated onto SS substrate to fabricate thin films (see Experimental Section for detailed procedures). However, when used as the anode for Li-ion cells, the free-standing CNT-SiNP film had a large irreversible capacity for the first cycle and poor cycling performance (see Figure S3). Previous studies using pure CNTs as anode for lithium ion batteries all found a very high irreversible capacity (>1200 mAh/g) for the first cycle.[33−36] This is because that majority of reaction of Li^+ with CNT surfaces are irreversible.[33] The poor cycling performance may also be due to the loose contact between CNTs and SiNPs. To overcome these issues, we have performed a short-time SiH_4 CVD to coat the CNTs and SiNPs with a thin layer of a-Si, which fuses all the CNTs and SiNPs together to form an integrated film. After a short time (~5 min) of CVD treatment, the CNT-SiNP film no longer showed a large irreversible capacity and good battery performance was obtained. Figure 4a and b show the SEM images of a CNT-SiNP film before and after SiH_4 CVD treatment. We believe the deposited a-Si had passivated the surface of CNTs, and the irreversible reaction with Li^+ was, thus, greatly reduced.

Figure 4c shows the cycling of a mixed CNT-SiNP film treated with SiH_4 CVD at a rate of C/10. In this film the SiNPs contribute more than 90% of the overall Si content. Only a small amount of SiH_4 CVD was needed to coat the CNTs with a-Si and to fuse the SiNPs and CNTs together. With the incorporation of SiNPs, the cell still demonstrated good Coulombic efficiency and had a capacity retention of 75% after 50 cycles, showing slightly faster decay compared to the film whose Si content is all a-Si. Figure 4d is the voltage profile of a half cell using free-standing CNT-SiNP film treated with SiH_4 CVD as the working electrode. The first charge has a short plateau at ~0.18 V due to the lithiation potential of pure a-Si deposited from SiH_4 CVD. Then, a second long plateau appears at 0.09 V, which is the lithiation potential of pure c-Si from SiNPs.[15,32] After the first charge, the profiles of the rest cycles show typical behavior of Li intercalating with amorphous Li_xSi, similar to those in Figure 3d.

CNT-Si Films after Battery Cycling. We also investigated the morphology of free-standing CNT-Si film without SiNPs after battery cycling. Figure 5 displays the SEM images of the free-standing CNT-Si film after different number of cycles. Figure 4a is a SEM image of the CNT-Si film after 10 cycles, which does not show significant breaking or pulverization. Previous studies on sputtered-on Si films all observed severe pulverization after several cycles.[27−30] Islands and aggregates of Si particles were found on the substrates after a few battery cycles.[27,28] In Figure 5a, ripples caused by repeated

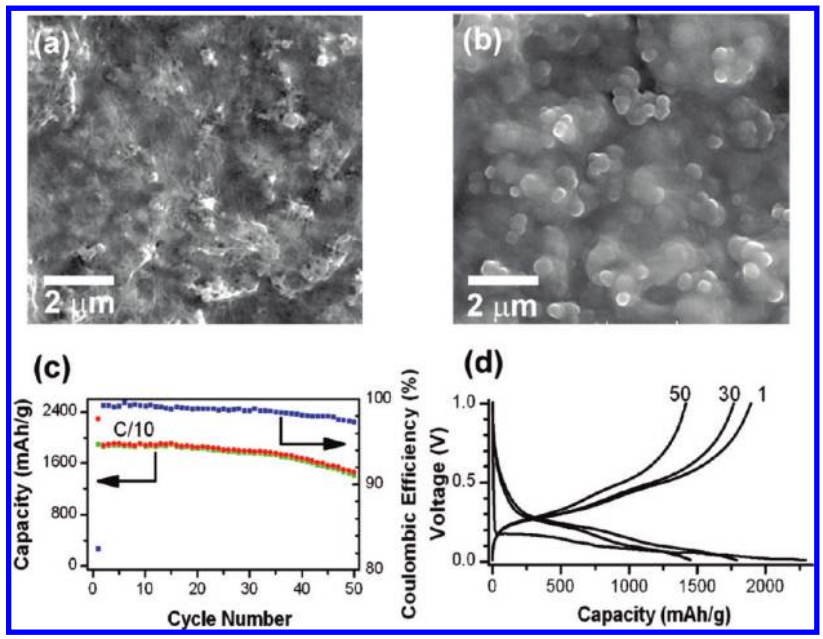

Figure 4. (a) SEM image of a CNT-SiNP composite film. (b) SEM image of a CNT-SiNP film after SiH_4 CVD treatment. (c) Charge (red) and discharge (green) capacity and Coulombic efficiency (blue) *versus* cycle number for a half cell using a silane VCD-treated CNT-SiNP film as working electrode cycled between 1−0.01 V. (d) Voltage profile of the cell in (c).

Si expansion and contraction during Li^+ intercalation can be clearly seen in the image. We believe the formation of ripples can relax the large strain in the film during Li^+ cycling thus reduce the breaking of the film. This demonstrates the advantage of free-standing CNT-Si film over pure sputtered-on Si film, which will endure significant pulverization upon Li^+ cycling. Figure 5b is a zoom-in SEM image of Figure 5a. Repeated Li^+ insertion and extraction still causes some damage to the film, and the formation of small Si bumps can been seen on the surface. The inset graph in Figure 5b is a SEM image taken at a broken edge of the CNT-Si film after 10 cycles, where CNTs sticking out of the edge can clearly be seen. Figure 5c is a SEM image of the composite film after 20 cycles. There appears to be more breaking on the film compared to the 10 cycle image. Figure 5d is a

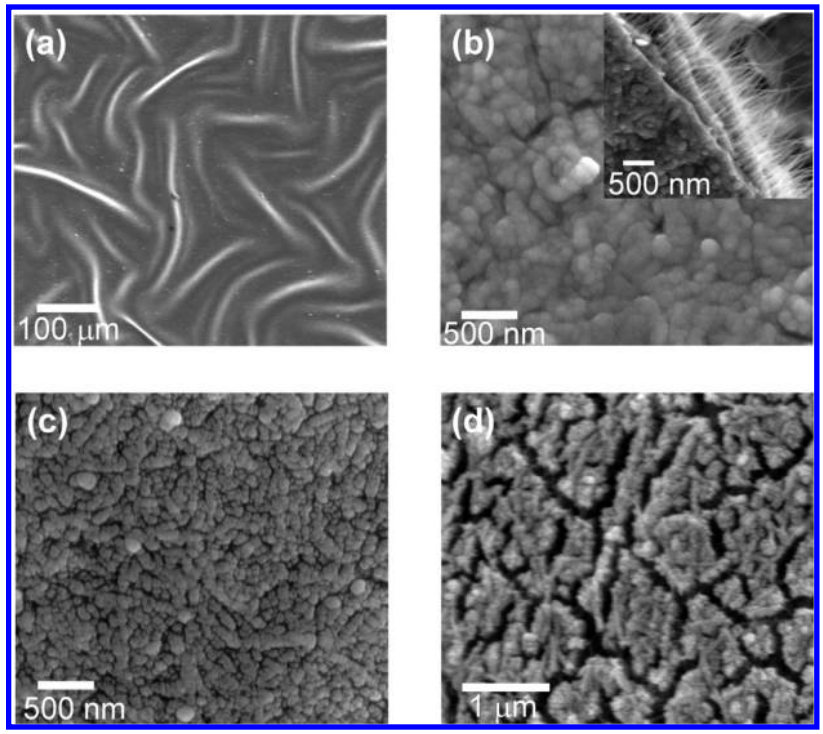

Figure 5. (a) SEM image of CNT-Si film after 10 cycles. Strain induced ripples can be cleanly seen. (b) Zoom-in SEM image of film in (a). Inset is a SEM image at a broken edge. (c) SEM image of CNT-Si film after 20 cycles. (d) SEM image of CNT-Si film after 40 cycles.

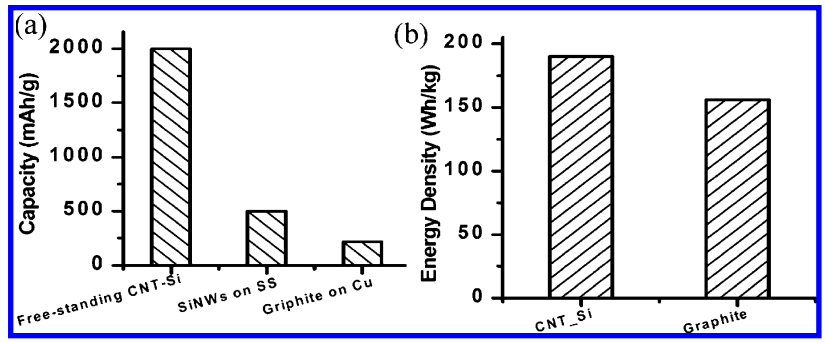

Figure 6. (a) Specific capacity for different anode systems, including the mass of the electrode material and the current collector. (b) Specific energy density comparison at whole battery level, including all the device components.

SEM image of the CNT-Si film after 40 cycles, where small cracks can be seen on the surface. However, the film did not disintegrate because the CNT network still connected the Si islands together. This proves the advantage of our CNT-Si composite film over pure Si films.

Comparison with Previous Results. To effectively increase the energy density on the device level, one needs to decrease the weight of each component. Previously, we have demonstrated that SiNWs on SS can offer 10 times the capacity compared to commercial graphite. However, the weight of the metal current collector on the anode side is more than that of the active material; therefore, the improvement of the energy density on the anode side will be significantly compromised. Here we replace the heavy metal current collector of ~10 mg/cm^2, with CNT film of ~0.2 mg/cm^2. Furthermore, the high capacity anode material, Si, was incorporated into such porous CNT films to form bifunctional, free-standing films. Such CNT-Si films greatly improve 10 times the specific capacity of anodes even when the weight of current collector is considered. Figure 6a shows the comparison of free-standing CNT-Si film, SiNWs on SS, and graphite on copper (Table S1; see SI materials and methods for details). It is clear that bifunctional CNT-Si dramatically increase the specific capacity when the weights of all components in anode side are counted. Such a huge weight saving on the anode side, including the current collector, would lead to 20% energy density increase in whole battery level (Figure 6b and Table S2; see SI materials and methods for details).

CONCLUSIONS

In conclusion, free-standing CNT-Si films up to 4 μm in thickness were synthesized by CVD deposition of a-Si on CNT films or by CNT-SiNP compositing technique. Such free-standing films successfully integrated the current collector and anode active material into a single sheet of film. The bifunctional films have low sheet resistance due to the infiltrated CNT network and high energy capacity due to the use of Si as anode material. High specific charge storage capacity, ~2000 mAh/g, and good cycling performance, much superior to pure sputter-on Si film with similar thickness, have been demonstrated. The great performance is attributed to the good mechanical strength and conductivity of the composite film, which can maintain structural integrity upon repeated lithium insertion and extraction. The CNT-Si film is still connected by a CNT network, where even small breaking or cracks appear in the film after cycling. The film was found to form "ripples" after lithium cycling due to the large strain in Si. Furthermore, the bifunctional CNT-Si film, when compared to the graphite anode on Cu current collector, can significantly decrease the weight percentage of the anode side in Li-ion batteries from ~20% to ~2%. Therefore, the integrated structure effectively increases the specific capacity by 10 times on the anode side and the energy density by 20% at the whole battery level. With the high capacity, low weight of the CNT-Si anode, further improvement of the energy density of the Li-ion battery will solely depend on the improvement of the cathode side.

EXPERIMENTAL SECTION

CNT Films On SS 500 Mesh. CNT ink in water was prepared by dispersing purified CNTs in water with SDBS surfactant. The concentration of CNT is 1.6 mg/mL and of SDBS is 10 mg/mL. After bath sonication for 5 min, the CNT dispersion was probe-sonicated for 30 min at 200 W (VC 505; Sonics) to form an ink. To form a standing CNT membrane on SS mesh, a 500 mesh was dipped into a CNT ink, taken out, and dried in an oven at 65 °C. The SS mesh supported CNT film was then used to be deposited with Si.

Free-Standing CNT and CNT-SiNP Thin Films. A total of 10 mL of CNT ink was spread out onto a stainless steel substrate with the Meyer rod coating method. The wet film was then slowly dried at 60 °C to avoid bubbling. The dried film was carefully rinsed with DI water to remove the surfactants. Due to the poor adhesion between the CNT film and the stainless substrate, the CNT film can be easily peeled off from the substrate, floated on DI water, and picked up with a metal mesh. The final free-standing CNT film was obtained after drying the wet film on the metal mesh. Then silicon was deposited onto the free-standing CNT film using the CVD process. For CNT-Si NP ink, 1.6 mg/mL CNT and 10 mg/mL Si NP were dispersed in water with 10 mg/mL SDBS. The dispersion was then probe-sonicated for 10 min before use. The fabrication procedures for the CNT-Si NP films were the same as those for the aforementioned CNT films.

Silane CVD. Obtained SS mesh supported CNT film, free-standing CNT film, or free-standing CNT-SiNP films were cut into 1 × 1 cm small pieces and loaded into a chemical-vapor-deposition (CVD) tube furnace. The furnace was pumped to vacuum, purged with pure argon, and then heated to 500 °C. The CNT and CNT-SiNP films were annealed at 500 °C for 40 min to remove the absorbed surfactant. After annealing, a compressed gas of 2% silane balanced in argon was flowed to produce a-Si deposition onto these free-standing films. Flow rates between 50 and 100 sccm were used for the delivery of SiH_4/Ar gas. The pressure inside the furnace was set between 40 and 100 Torr during CVD process. The total CVD time was 5−60 min. The amount of a-Si deposition can be controlled by varying the CVD time, the partial pressure of SiH_4, and the flow rate. The weights of the CNT films or CNT-SiNP films before and after annealing and after a-Si deposition were accurately measured using a microbalance (Sartarious SE2, 0.1 μg resolution).

Cell Fabrication and Testing. To test the battery performance of our various free-standing films, pouch type half cells were made using free-standing films as the working electrode, Celgard 2250 separator, and Li metal foil as counterelectrode. The electrolyte was 1.0 M $LiPF_6$ in 1:1 w/w ethylene carbonate/diethyl carbonate (Ferro Corporation). The cells were assembled inside an Ar-filled glovebox and sealed in aluminized polyethylene laminate bags. Galvanostatic measurements were made using a Biologic VMP3 multichannel system. The C−Si NW electrodes were cycled between 1 and 0.01 V.

Material Charaterization. The free-standing films were characterized by an FEI Sirion scanning electron microscope (SEM) and a Philips CM20 transmission electron microscope (TEM). Delithiated film electrodes after cycling were took out of the cell bags inside a glovebox, washed with acetonitrile (ACN) and 0.2 M HCl to remove the residual electrolyte and lithium salts, and dried at room temperature before further SEM and TEM investigation.

Acknowledgment. The work is partially supported by King Abdullah University of Science and Technology Investigator Award KUS-I1-001-12 (to Y.C.).

Supporting Information Available: Detailed experimental method, additional SEM images, and cycling performance. This material is available free of charge *via* the Internet at http://pubs.acs.org.

REFERENCES AND NOTES

1. Kasavajjula, U.; Wang, C. S.; Appleby, A. J. Nano- and Bulk-Silicon-Based Insertion Anodes for Lithium-Ion Secondary Cells. *J. Power Sources* **2007**, *163*, 1003–1039.
2. Green, M.; Fielder, E.; Scrosati, B.; Wachtler, M.; Moreno, J. S. Structured Silicon Anodes for Lithium Battery Applications. *Electrochem. Solid-State Lett.* **2003**, *6*, A75–A79.
3. Li, H.; Huang, X. J.; Chen, L. Q.; Zhou, G. W.; Zhang, Z.; Yu, D. P.; Mo, Y. J.; Pei, N. The Crystal Structural Evolution of Nano-Si Anode Caused by Lithium Insertion and Extraction at Room Temperature. *Solid State Ionics* **2000**, *135*, 181–191.
4. Zhang, X. W.; Patil, P. K.; Wang, C. S.; Appleby, A. J.; Little, F. E.; Cocke, D. L. Electrochemical Performance of Lithium Ion Battery, Nano-Silicon-Based, Disordered Carbon Composite Anodes with Different Microstructures. *J. Power Sources* **2004**, *125*, 206–213.
5. Liu, W. R.; Guo, Z. Z.; Young, W. S.; Shieh, D. T.; Wu, H. C.; Yang, M. H.; Wu, N. L. Effect of Electrode Structure on Performance of Si Anode in Li-Ion Batteries: Si Particle Size and Conductive Additive. *J. Power Sources* **2005**, *140*, 139–144.
6. Zhang, T.; Gao, J.; Zhang, H. P.; Yang, L. C.; Wu, Y. P.; Wu, H. Q. Preparation and Electrochemical Properties of Core-Shell Si/SiO Nanocomposite as Anode Material for Lithium Ion Batteries. *Electrochem. Commun.* **2007**, *9*, 886–890.
7. Mao, O.; Turner, R. L.; Courtney, I. A.; Fredericksen, B. D.; Buckett, M. I.; Krause, L. J.; Dahn, J. R. Active/Inactive Nanocomposites as Anodes for Li-Ion Batteries. *Electrochem. Solid-State Lett.* **1999**, *2*, 3–5.
8. Mao, O.; Dunlap, R. A.; Dahn, J. R. Mechanically Alloyed Sn-Fe(-C) Powders as Anode Materials for Li-Ion Batteries. I. The Sn_2Fe-C system. *J. Electrochem. Soc.* **1999**, *146*, 405–413.
9. Kim, I.; Kumta, P. N.; Blomgren, G. E. Si/TiN Nanocomposites: Novel Anode Materials for Li-Ion Batteries. *Electrochem. Solid-State Lett.* **2000**, *3*, 493–496.
10. Kim, I. S.; Kumta, P. N. High Capacity Si/C Nanocomposite Anodes for Li-Ion Batteries. *J. Power Sources* **2004**, *136*, 145–149.
11. Yoshio, M.; Kugino, S.; Dimov, N. Electrochemical Behaviors of Silicon Based Anode Material. *J. Power Sources* **2006**, *153*, 375–379.
12. Yang, J.; Wang, B. F.; Wang, K.; Liu, Y.; Xie, J. Y.; Wen, Z. S. Si/C Composites for High Capacity Lithium Storage Materials. *Electrochem. Solid-State Lett.* **2003**, *6*, A154–A156.
13. Lee, H. Y.; Lee, S. M. Graphite-FeSi Alloy Composites as Anode Materials for Rechargeable Lithium Batteries. *J. Power Sources* **2002**, *112*, PII S0378−7753(02)00461−5.
14. Kim, B. C.; Uono, H.; Satou, T.; Fuse, T.; Ishihara, T.; Ue, M.; Senna, M. Cyclic Properties of Si-Cu/Carbon Nanocomposite Anodes for Li-Ion Secondary Batteries. *J. Electrochem. Soc.* **2005**, *152*, A523–A526.
15. Chan, C. K.; Peng, H. L.; Liu, G.; McIlwrath, K.; Zhang, X. F.; Huggins, R. A.; Cui, Y. High-Performance Lithium Battery Anodes Using Silicon Nanowires. *Nat. Nanotechnol.* **2008**, *3*, 31–35.
16. Cui, L. F.; Yang, Y.; Hsu, C. M.; Cui, Y. Carbon-Silicon Core-Shell Nanowires as High Capacity Electrode for Lithium Ion Batteries. *Nano Lett.* **2009**, *9*, 3370–3374.
17. Kim, H.; Seo, M.; Park, M. H.; Cho, J. A Critical Size of Silicon Nano-Anodes for Lithium Rechargeable Batteries. *Angew. Chem., Int. Ed.* **2010**, *49*, 2146−2149.
18. Park, M. H.; Kim, M. G.; Joo, J.; Kim, K.; Kim, J.; Ahn, S.; Cui, Y.; Cho, J. Silicon Nanotube Battery Anodes. *Nano Lett.* **2009**, *9*, 3844–3847.
19. Hu, L.; Yang, J. C. Y.; Jeong, S.; La Manita, F.; Cui, L.; Cui, Y. Highly Conductive Paper for Energy-Storage Devices. *Proc. Natl. Acad. Sci. U.S.A.* **2009**, *106*, 21490.
20. Cao, Q.; Kim, H. S.; Pimparkar, N.; Kulkarni, J. P.; Wang, C. J.; Shim, M.; Roy, K.; Alam, M. A.; Rogers, J. A. Medium-Scale Carbon Nanotube Thin-Film Integrated Circuits on Flexible Plastic Substrates. *Nature* **2008**, *454*, 495–U4.
21. Gruner, G. Carbon Nanotube Films for Transparent and Plastic Electronics. *J. Mater. Chem.* **2006**, *16*, 3533–3539.
22. Hu, L. B.; Gruner, G.; Li, D.; Kaner, R. B.; Cech, J. Patternable Transparent Carbon Nanotube Films for Electrochromic Devices. *J. Appl. Phys.* **2007**, *101*, 1–8.
23. Zhang, D. H.; Ryu, K.; Liu, X. L.; Polikarpov, E.; Ly, J.; Tompson, M. E.; Zhou, C. W. Transparent, Conductive, and Flexible Carbon Nanotube Films and Their Application in Organic Light-Emitting Diodes. *Nano Lett* **2006**, *6*, 1880–1886.
24. Wu, Z. C.; Chen, Z. H.; Du, X.; Logan, J. M.; Sippel, J.; Nikolou, M.; Kamaras, K.; Reynolds, J. R.; Tanner, D. B.; Hebard, A. F.; Rinzler, A. G. Transparent, Conductive Carbon Nanotube Films. *Science* **2004**, *305*, 1273–1276.
25. Li, J.; Hu, L.; Wang, L.; Zhou, Y.; Gruner, G.; Marks, T. J. Organic Light-Emitting Diodes Having Carbon Nanotube Anodes. *Nano Lett* **2006**, *6*, 2472–2477.
26. Johnson, B. A.; White, R. E. Characterization of Commercially Available Lithium-Ion Batteries. *J. Power Sources* **1998**, *70*, 48.
27. Maranchi, J. P.; Hepp, A. F.; Kumta, P. N. High Capacity, Reversible Silicon Thin-Film Anodes for Lithium-Ion Batteries. *Electrochem. Solid-State Lett.* **2003**, *6*, A198–A201.
28. Yin, J. T.; Wada, M.; Yamamoto, K.; Kitano, Y.; Tanase, S.; Sakai, T. Micrometer-Scale Amorphous Si Thin-Film Electrodes Fabricated by Electron-Beam Deposition for Li-Ion Batteries. *J. Electrochem. Soc.* **2006**, *153*, A472–A477.
29. Ohara, S.; Suzuki, J. J.; Sekine, K.; Takamura, T. Attainment of High Rate Capability of Si Film as the Anode of Li-Ion Batteries. *Electrochemistry* **2003**, *71*, 1126–1128.
30. Komaba, S.; Mikami, F.; Itabashi, T.; Baba, M.; Ueno, T.;

Kumagai, N. Improvement of Electrochemical Capability of Sputtered Silicon Film Anode for Rechargeable Lithium Batteries. *Bull. Chem. Soc. Jpn.* **2006**, *79*, 154–162.
31. Cui, L. F.; Ruffo, R.; Chan, C. K.; Peng, H. L.; Cui, Y. Crystalline-Amorphous Core-Shell Silicon Nanowires for High Capacity and High Current Battery Electrodes. *Nano Lett.* **2009**, *9*, 491–495.
32. Obrovac, M. N.; Krause, L. J. Reversible Cycling of Crystalline Silicon Powder. *J. Electrochem. Soc.* **2007**, *154*, A103–A108.
33. Ng, S. H.; Wang, J.; Guo, Z. P.; Wang, G. X.; Liu, H. K. Single Wall Carbon Nanotube Paper as Anode for Lithium-Ion Battery. *Electrochim. Acta* **2005**, *51*, 23–28.
34. Shin, H. C.; Liu, M. L.; Sadanadan, B.; Rao, A. M. Lithium Insertion into Chemically Etched Multiwalled Carbon Nanotubes. *J. Solid State Electrochem.* **2004**, *8*, 908–913.
35. Sharon, M.; Hsu, W. K.; Kroto, H. W.; Walton, D. R. M.; Kawahara, A.; Ishihara, T.; Takita, Y. Camphor-Based Carbon Nanotubes as an Anode in Lithium Secondary Batteries. *J. Power Sources* **2002**, *104*, 148–153.
36. Zhao, J.; Gao, Q. Y.; Gu, C.; Yang, Y. Preparation of Multiwalled Carbon Nanotube Array Electrodes and its Electrochemical Intercalation Behavior of Li Ions. *Chem. Phys. Lett.* **2002**, *358*, 77–82.